Chemical Engineering Journal 164 (2010) 261–266

Contents lists available at ScienceDirect

Chemical Engineering Journal

journal homepage: www.elsevier.com/locate/cej

Sono-synthesis of Mn_3O_4 nanoparticles in different media without additives

T. Rohani Bastami, M.H. Entezari*

Department of Chemistry, Ferdowsi University of Mashhad, 91775 Mashhad, Iran

ARTICLE INFO

Article history:
Received 15 March 2010
Received in revised form 12 August 2010
Accepted 13 August 2010

Keywords:
Hausmannite
Nanoparticle
Ultrasound
Aqueous medium
Olive oil
Almond oil
Paraffin

ABSTRACT

Hausmannite (Mn_3O_4) nanoparticles were prepared by ultrasound in various media for the first time under ambient conditions without any additives. The synthesis was carried out by direct sonication of manganese acetate in water. The nanoparticles with high crystallinity and sizes less than 4 nm appeared after 3 min of sonication. Water in oil emulsion was selected as another medium for the synthesis. In this case, the water phase containing manganese acetate was dispersed into the oil phase. Two different types of oil were chosen as a medium for the synthesis—paraffin as a mineral oil; olive and almond as vegetable oils. In all selected media, hausmannite was prepared with different sizes, shapes, and crystallinity. In the vegetable oils, the nanoparticles were larger than the nanoparticles prepared in water but the crystallinity was lower than in the water phase. In contrast, the crystallinity of the product in mineral oil was higher than in vegetable oil and lower than in water but the particle size in mineral oil was larger than the two other media. TEM (transmission electron microscopy) and XRD (X-ray diffraction) were used for characterizing the products. The XRD patterns confirmed that different media yielded to the same product, Mn_3O_4 nanoparticle. The TEM images showed that the size and shape of nanoparticles were different in the different media. In vegetable oil, nanoparticles had a spherical shape with maximum ~7 nm in size. Using mineral oil, the shape of nanoparticles was diamond form and maximum ~50 nm in size. In water phase, the size of nanoparticle is less than ~4 nm with spherical shape.

1. Introduction

Nanotechnology as a field of applied science has been focused on the design, synthesis, characterization and application of nanomaterials. This branch of knowledge is a sub-classification of technology in colloidal science, biology, physics, chemistry and other scientific fields and involves the study of phenomena and manipulation of materials in the nanoscale [1,2]. The properties of transition metal oxide nanoparticles are different from those of the bulk materials in many areas such as optical, magnetic, and electrical properties [3–5]. Sonochemistry as an effective and powerful technique is used for the synthesis of different compounds under normal conditions (ambient pressure and temperature). Acoustic cavitation is responsible for the physical and chemical changes during the sonication [6,7]. The chemical effects of ultrasound were explored for many years [6]. Ultrasonic irradiation of aqueous solution leads to hydrogen and hydroxyl radicals [8,9]. These radicals can recombine to return to their original form or combine to produce H_2 and H_2O_2. They can also produce $HO_2^{\bullet}$ and other radicals with different combinations. These types of radicals act as strong oxidants and reductants in different sonochemical reactions. Physical effects of ultrasonic waves such as the enhancement of mass transfer, induction of primary nucleation at lower supersaturation, shortening the induction time and chemical effects such as radical formation through cavitation can affect on the crystallization process. Suslick et al. [10,11] prepared unusual nanostructure materials by using some volatile organic liquids. Recently, this technique provides a new approach for the synthesis of nanostructure materials [12–18].

In addition, this method has many advantages not found with conventional methods. Under sonication, it is possible to synthesize the nanoparticles in normal conditions without additives, and avoiding calcinations at high temperatures [19]. Transition metal oxides in the form of nanomaterials have prepared by ultrasonic methods [20–23]. Manganese oxide nanoparticles have been synthesized by many methods. There are different forms of manganese oxide such as MnO, MnO_2, Mn_2O_3, MnOOH, and Mn_3O_4 [24]. Hausmannite as a brown to black metallic mineral is a complex oxide containing both di- and tri-valent manganese. The formula can be represented as $Mn^{2+}(Mn^{3+})_2O_4$, Mn^{3+} in an octahedral position and Mn^{2+} in a tetrahedral position of the spinel structure. Mn_3O_4 has different applications in industry such as applying as a catalyst for oxidation of CH_4, for the reduction of nitrobenzene, for the decomposition of waste NO_x [25–28], and the oxidation of C3 organic compounds like: propane, propene, acetone and acrolein [29].

* Corresponding author.
E-mail address: moh_entezari@yahoo.com (M.H. Entezari).

1385-8947/$ – see front matter © 2010 Elsevier B.V. All rights reserved.
doi:10.1016/j.cej.2010.08.030

Several methods were used for the synthesis of Mn_3O_4 nanoparticles with different sizes and shapes. Reflux of hydrated manganese hydroxide at 100 °C produced Mn_3O_4 with the average particle size of 50 nm [30]. A hydrothermal method was performed under normal condition at different pH values, leading to the formation of Mn_3O_4 at higher pH and formation of γ-MnOOH nanowire at lower pH [31]. Mixing of manganese nitrate and hexamethylenetetramine solutions at different temperatures between 20 and 80 °C resulted in 18–41 nm Mn_3O_4 nanoparticle [32]. Benzyl alcohol with two precursors of potassium permanganate and manganese acetylacetonate led to the formation of Mn_3O_4 and MnO as the dominant phases [33]. Mn_3O_4 nanoparticles in the range of 10–20 nm were obtained by using the metallic salt and hydrazine [34]. Hausmannite nanoparticles with spherical shape and particle diameter of 35 nm were synthesized at low temperature by using starch as capping agent [35]. Sonochemical method on different salts of manganese(II) was applied at pH = 8.3 and led to particle sizes between 30 and 80 nm which was depended on the type of salt [36].

The aim of the current research is the synthesis of manganese oxide nanoparticle (hausmannite) under normal conditions in different media with ultrasonic waves. Aqueous solutions of manganese acetate(II), and the dispersion of aqueous phase containing manganese salt in different oils were used for this synthesis.

2. Experimental

2.1. Materials

Paraffin liquid and manganese(II) acetate, $4H_2O$ were purchased from Merck Company. Olive and almond oils with high purity were purchased from local market and n-hexane as a solvent for washing the particles from the oil phase was from Fluka. Distilled water was used with a resistivity about 0.33 MΩ cm.

2.2. Instruments

The ultrasonic irradiation was carried out with equipment operating at 20 kHz (XL-2020, Misonix, 550 W). The X-ray of product was recorded on Bruker, D8ADVANCE, Germany (X-Ray Tube Anode: Cu, Wavelength: 1.5406 Å (Cu Kα) Filter: Ni). The morphology and size of the particles were characterized by transmission electron microscopy (TEM, LEO 912 ab, Zeiss Germany, 120 kV).

2.3. Procedure

2.3.1. Synthesis of manganese oxide in aqueous medium

Manganese acetate was used as a precursor for this synthesis and 4.6 g of this compound was dissolved in distilled water (30 mL). This solution was poured in a 100 mL beaker as a sonochemical reaction vessel and then sonicated. A small amount of water was added to the reaction vessel during the sonication to compensate for the loss of evaporated water. The temperature was raised and reached to about 80 °C after 6 min. The reaction products were centrifuged, washed with distilled water and dried at 100 °C. Only one experiment was run under these same mentioned conditions with an Ar atmosphere in neutral pH and sonicated for 45 min. The other experiments were carried out in neutral pH and air atmosphere at the same temperature. For the comparison, one experiment was designed as a control by using a stirrer 500 rpm instead of ultrasonic waves and other conditions were the same as in the ultrasonic experiments. But, the time of procedure was 3 h.

2.3.2. Synthesis of manganese oxide in emulsion medium

In this part of experiment, 4 mL of saturated solution of $Mn(OAc)_2$ and 30 mL of oil were added in a 100 mL beaker. The two immiscible phases were uniformed and the emulsion was established by sonication of solution at initial temperature of 20 °C. The temperature of immersed vessel in an ice bath was increased to about 73 °C during the initial 5 min and then by removing the ice bath, the temperature was raised to about 95 °C. The position of probe was fixed by its immersion to 1 cm in the initial oil phase. The sonication was continued to 35, 20, and 17 min for paraffin, almond oil and olive oil, respectively. The reaction products were centrifuged at 15000 rpm for 20 min and then washed with n-hexane and boiled water many times to remove the oil phase from the solid particles. Finally, the solid particles were dried at 100 °C. These experiments were also carried out in an air atmosphere.

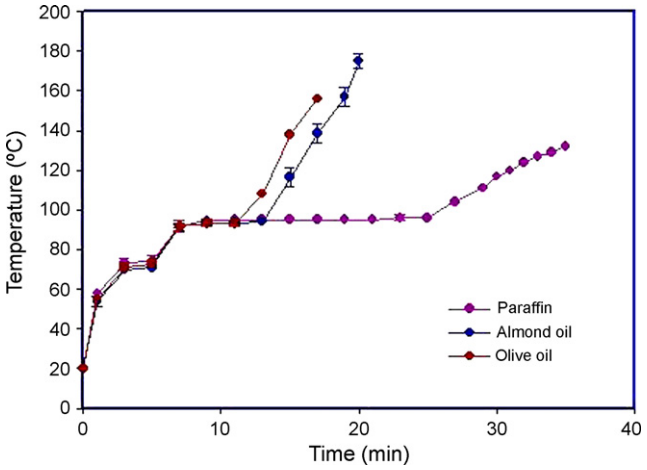

Fig. 1. Temperature versus sonication time (4 ml of distilled water + 30 ml of oil).

In addition, two sets of experiment were designed to study of temperature changes versus time during the process. One of them is the mixture of 4 mL of saturated solution of $Mn(OAc)_2$ and 30 mL of oil, and another one is the mixture of 4 mL of distilled water with 30 mL of oil. In both experiments, the sonication time for paraffin, almond, and olive oil were 35, 20, and 17 min, respectively. Initial temperature was 20 °C in all cases. Vessel was immersed in ice bath just for initial 5 min and then removed and the position of the probe was the same as mentioned above. Results are shown in Figs. 1 and 2. The physicochemical properties of the liquids and

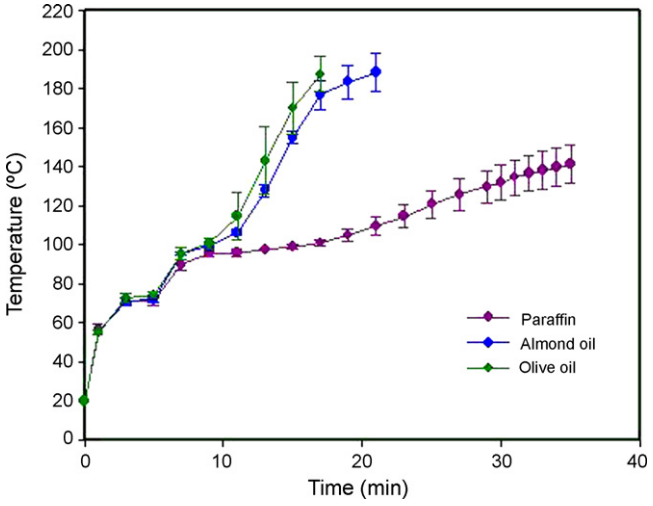

Fig. 2. Temperature versus sonication time (4 ml saturated solution of manganese acetate + 30 ml oil).

Table 1
Physicochemical parameters of liquids.

Liquid	Density (kg m^{-3}) 25 °C	Viscosity (cp) 25 °C	Acidity	Peroxide value (mequiv. O_2/kg)	Iodine value (g I_2/100 g)	Water and volatile content %(10^3 °C)
Water	995.7	1.002	–	–	–	–
Olive oil	913.2	61.39	0.53	8.9	82.6	<0.1
Almond oil	920.2	52.83	0.6	0.5	97.9	<0.1
Paraffin	877.2	77.66	–	–	–	–

chemical analysis of vegetable oils are given in Tables 1 and 2, respectively.

3. Results and discussion

3.1. Proposed mechanism

Aqueous solutions of manganese(II) salts in the presence of strong bases form the pink-colored, insoluble manganese(II) hydroxide, $Mn(OH)_2$. In the presence of air and oxygen, $Mn(OH)_2$ is gradually oxidized to form dark-brown products which contain $Mn(OH)_3$ or possibly MnO, and $MnO_2{\cdot}nH_2O$. Manganese(II) hydroxide is a fairly weak base and when heated in air, it forms Mn_3O_4 [24].

In the case of sonication, the chemical reactions driven by intense ultrasonic waves can occur in three different regions [37,38]: (a) the inner environment of the collapsing bubble (gas phase), where high temperatures (several thousands of degrees) and pressures (hundreds of atmospheres) are produced and causing the pyrolysis of water into H and OH radicals, (b) the interfacial region between the cavitation bubbles and bulk solution, and (c) the bulk of the solution. The temperature in case (b) is lower than that in case (a) but, the temperature is still high enough to rupture chemical bonds. In the bulk solution, the reaction between reactant molecules and OH or H radicals produced by the cavitation can take place at the medium temperatures.

In this study, the nanoparticles were obtained without any basic additives. For finding the role of oxygen, the sono-synthesis of Mn_3O_4 nanoparticles was done in neutral pH under Ar atmosphere and this experiment did not lead to any product. Therefore, oxygen is necessary for the synthesis of Mn_3O_4 nanoparticles. In addition, there was a negligible amount of product in control method when the synthesis was carried out under an air atmosphere. It is known that the sonochemical reaction does not occur inside the cavity which is due to the ionic structure of initial components (manganese acetate). Therefore the reaction can facilitate in interface of the bubble or in the bulk of the solution. A suggested mechanism for the formation of Mn_3O_4 from aqueous manganese acetate in the presence of O_2 molecules are as following:

$$Mn(CH_3COO)_2 + 2H_2O \rightarrow Mn(OH)_2 + 2CH_3COOH \quad (1)$$

$$H_2O \xrightarrow{)))))} H^\bullet + OH^\bullet \quad (2)$$

Table 2
Chemical analysis of olive and almond oils.

Olive oil			Almond oil		
Acid	CAN[a]	Conc%	Acid	CAN[a]	Conc.%
Palmitic	16:0	12.67	Palmitic	16:0	5.5
Palmitoleic	16:1	0.61	Palmitoleic	16:1	0.2
Stearic	18:0	2.97	Stcaric	18:0	2.8
Oleic	18:1	71.01	Oleic	18:1	70
Linoleic	18:2	10.40	Linoleic	18:2	21
Linolenic	18:3	0.58	Linolenic	18:3	0.1
Eicosenoic	20:1	0.29	Eicosenoic	20:1	0.1
Arachidonic	20:4	0.14	Behenic	22:0	0.1

[a] Carbon atom number.

According to Okitsu et al. [39], OOH radicals are formed by the reaction of H radicals with O_2 molecules under the air atmosphere and then the recombination of OOH radicals proceed to form H_2O_2:

$$H^\bullet + O_2 \rightarrow {}^\bullet OOH \quad (3)$$

$$2{}^\bullet OOH \rightarrow H_2O_2 + O_2 \quad (4)$$

The oxidant generated by ultrasound can initiate the oxidation of $Mn(OH)_2$:

$$3Mn(OH)_2 + H_2O_2 \rightarrow Mn_3O_4 + 4H_2O \quad (5)$$

It should be mentioned that, the synthesis of Mn_3O_4 in neutral medium without sonication leads to a negligible amount of product after 3 h.

3.2. Temperature versus time of sonication in different media

Fig. 1 shows the effect of sonication time on the temperature of a mixture containing 4 mL of distilled water dispersed in 30 mL of oil (paraffin, olive, and almond oils). Results indicate that the increase of temperature is slower for paraffin than for the two other vegetable oils. In addition, the temperature was constant for a longer time for paraffin than for the two other oils at 95 °C which is due to the evaporation of the dispersed phase (water) from the oil phase. After complete evaporation of the water, the mixture changed from a milky emulsion to a suspension containing solid particles. Three reasons may be claimed for the behaviors of temperature versus time of sonication in different media. One is related to the heat capacity of the medium which is higher for paraffin than for the two other oils [40], and the second is related to the viscosity which is also higher for paraffin. Viscosity for paraffin, olive, and almond oil are 77.66, 61.39, and 5283 cp, respectively (Table 1). The third one may be related to the cavitation process which occurs more easily in a medium with lower viscosity. Due to the lower viscosity of olive and almond oils and higher activity of cavitation process in these media, the number of cavities should be higher. Therefore, the evaporation of water is faster and easier in these media than in paraffin and a shorter time is required for the total evaporation of water from the mixture.

Fig. 2 shows temperature versus sonication time for the dispersion of saturated solution of manganese acetate (4 mL) in 30 mL of oil. As it is shown, the rise of temperature is different from that in Fig. 1. The temperature was not constant during the evaporation of water from dispersed solution and increased gradually. In addition, loss of water phase from the solution in Fig. 2 occurred at higher temperature than in Fig. 1. These differences are due to the presence of salt in distilled water. The concentration of solution was increased during the evaporation and led to a higher boiling point and therefore, the temperature was increased gradually. Another difference is related to the final temperature and time of product formation. Paraffin as a mineral oil has a final temperature lower than the vegetable oils (almond and olive oils). The product appeared after 2 min in paraffin and after 10–12 min in vegetable oils. This behavior may be attributed to the higher viscosity and lower density of paraffin (Table 1). The difference of densities between water and paraffin are greater than water and the two other oils. In addition, the viscosity of paraffin is higher than

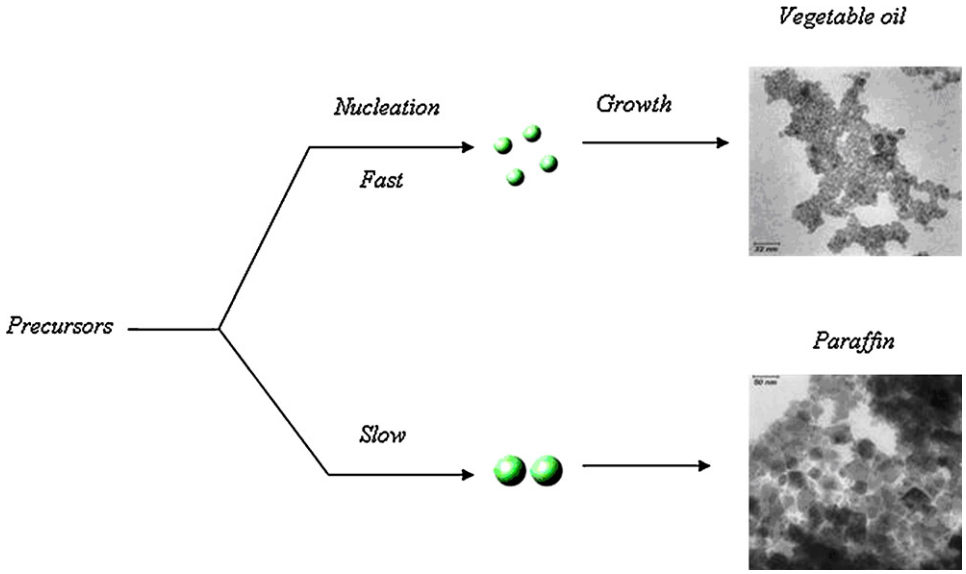

Scheme 1. Schematic representation of nanocrystal synthesis.

the two other oils. The densities of water, paraffin, olive oil, and almond oil are 995.7, 877.2, 913.2, and 920.2 kg m^{-3}, respectively. Therefore, the resistance to mix of two phases is different. Sonication under the same conditions can emulsify water in vegetable oils easier than the water in mineral oil. It seems that the droplet size of water in paraffin should be larger than water in vegetable oils under the same conditions. If the water droplet in oil phase assumes as a reactor, larger droplet has higher amount of salt and can lead to an observable particle in a shorter time.

According to the nucleation theory, the increase of temperature leads to an increase of nucleation rate [41,42]. As it is shown in Fig. 2, the induction period for mineral and vegetable oils were occurred at 70 and 107 °C, respectively. Therefore, the temperature of reaction in vegetable oil is higher than the mineral oil. This means that the nucleation rate is higher in vegetable oil than mineral one. Therefore, a fast nucleation resulted in the generation of a larger number of seed nuclei and yields to smaller nanoparticles (see Scheme 1).

Cavitation also plays an important role in the increase of nucleation rate. As it was mentioned, the cavitation process occurs more easily in the vegetable oils than in mineral oil due to its lower viscosity. Therefore, the number of cavitation bubbles and possible nucleation sites for crystallization can be increased.

In aqueous solution the product appeared in about 5–7 min and the temperature reached about 80 °C after 6 min. The temperature was self-maintained at about 80 °C until the end of the reaction.

3.3. XRD results

The X-ray diffraction patterns of the samples prepared in different media under ultrasound are shown in Figs. 3 and 4. It is found that all the products are in agreement with the XRD pattern of hausmannite. The crystalline patterns are matched with the reported values for the tetragonal Mn_3O_4 phase (JCPDS; 24-734). The miller indices are exhibited in XRD patterns in Figs. 3 and 4. The calculated lattice parameters are also shown in Table 3. The XRD pattern related to the sample prepared in aqueous medium have the greater intensity than the others. The X-ray diffraction pattern for the sample synthesized in paraffin as an oil phase shows the sharper and higher peaks than olive and almond oils. The XRD patterns related to the olive and almond oils show lower intensity and wider peaks. This means that the samples prepared in aqueous and paraffin have higher crystallinity than the sample prepared in vegetable oils as a continuous phase. As it is shown in Figs. 1 and 2, the behavior of temperature versus sonication time is approximately the same for water dispersed in paraffin and for the water phase alone (Section 3.1). But, the behavior mentioned is the same for the two selected vegetable oils with high variation of temperature versus sonication time. The species can be crystallized at about constant temperature better than at the variable temperatures.

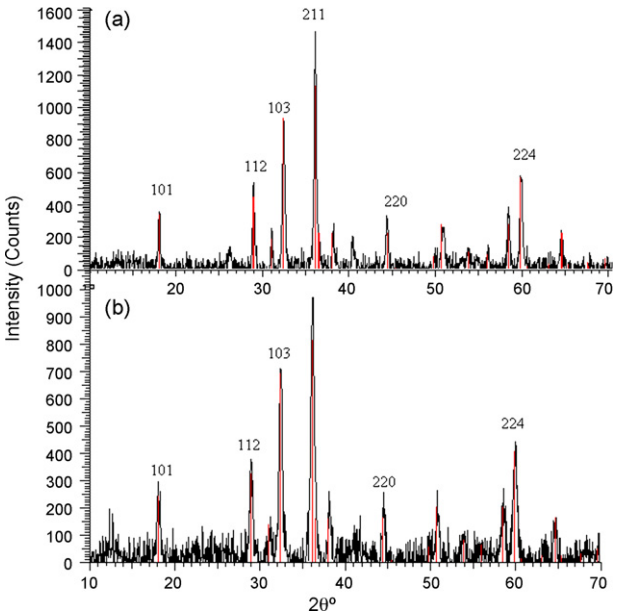

Fig. 3. X-ray diffraction patterns of the hausmannite synthesized in: (a) aqueous medium and (b) water/paraffin emulsion.

Table 3
Lattice parameters of Mn_3O_4.

Medium	a (Å)	c (Å)
Aqueous	5.76	9.44
W/paraffin	5.75	9.43
W/olive oil	5.75	9.46
W/almond oil	5.73	9.46

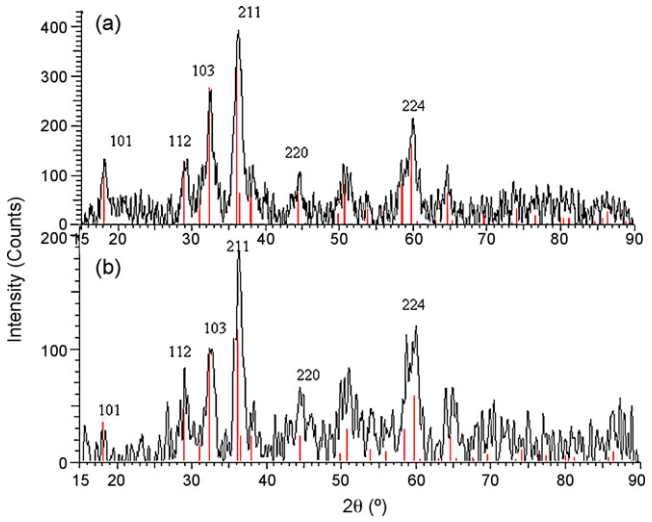

Fig. 4. X-ray diffraction patterns of the hausmannite synthesized in: (a) water/olive oil and (b) water/almond oil emulsions.

3.4. TEM results

Fig. 5 shows the TEM measurements of the sample prepared in aqueous medium. The picture shows that the nanocrystal is nearly spherical shape with very small size less than ~4 nm. Fig. 6 is related to the TEM micrographs of the sample synthesized in aqueous solution dispersed in paraffin as an oil phase. The nanocrystals are diamond shaped with sharp-edges and with the size in the range of 5–50 nm. Figs. 7 and 8 show the TEM micrographs of samples prepared in olive, and almond oil, respectively. According to these pictures, both samples exhibit spherical shape with sizes less than ~7 nm. The results show that the type of oil has an effect on the size and shape of nanoparticles. The sample prepared in vegetable oils as an oil phase shows spherical shape with maximum size of ~7 nm, but in mineral oil as an oil phase, the nanoparticle exhibits diamond shape with maximum size of 50 nm.

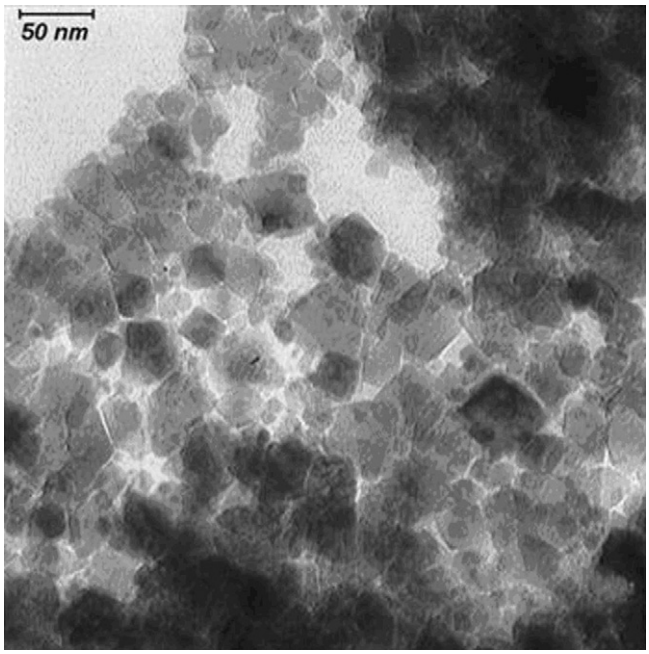

Fig. 6. TEM image of hausmannite (Mn_3O_4) (water/paraffin emulsion).

The reason for the change of the grain size in mineral oil and vegetable oil may be related to the nucleation rate and the growth of nanoparticles. According to Figs. 1 and 2, the rate of increase of temperature for vegetable oil is higher than for mineral oil. Therefore the nucleation rate of nanoparticles is higher in vegetable oil medium than in mineral oil. So, a higher rate of nucleation leads to a decrease of the average particle size. In contrast, in mineral oil the nucleation rate is lower and this leads to the larger grain size. The crystallinity of the product in paraffin is higher than vegetable oils which may be due to the stability of temperature during the crystallization in paraffin.

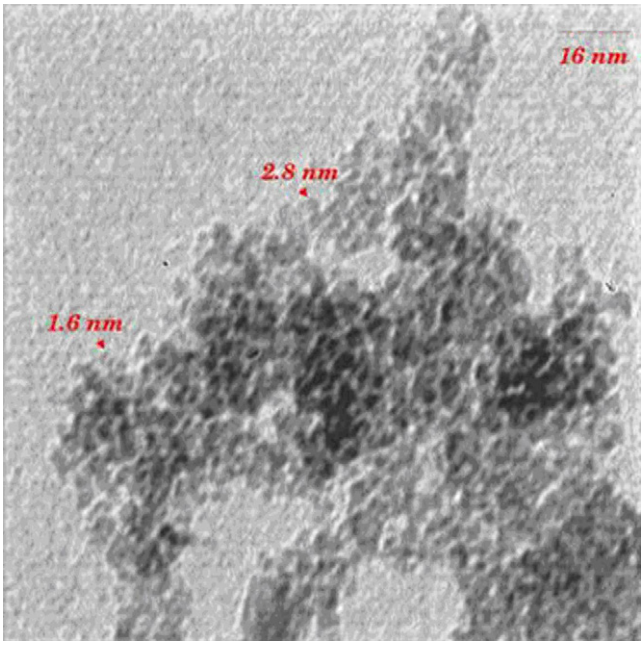

Fig. 5. TEM image of hausmannite (Mn_3O_4) (aqueous medium).

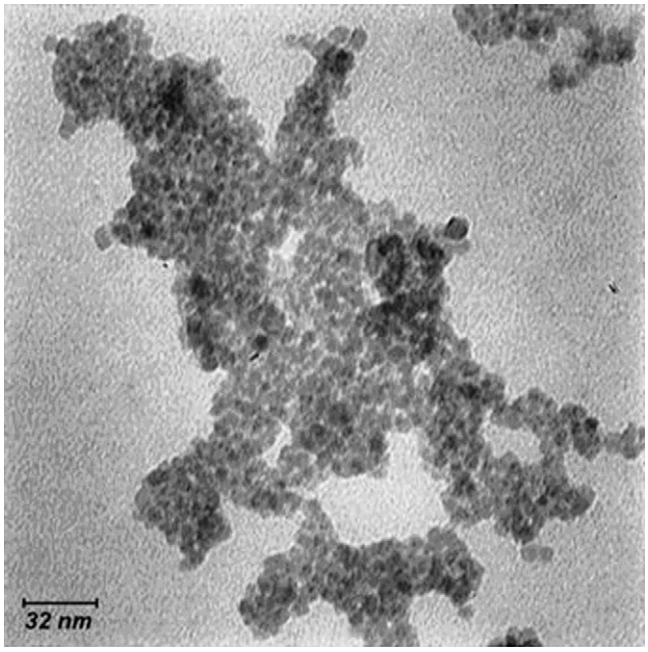

Fig. 7. TEM image of hausmannite (Mn_3O_4) (water/olive oil emulsion).

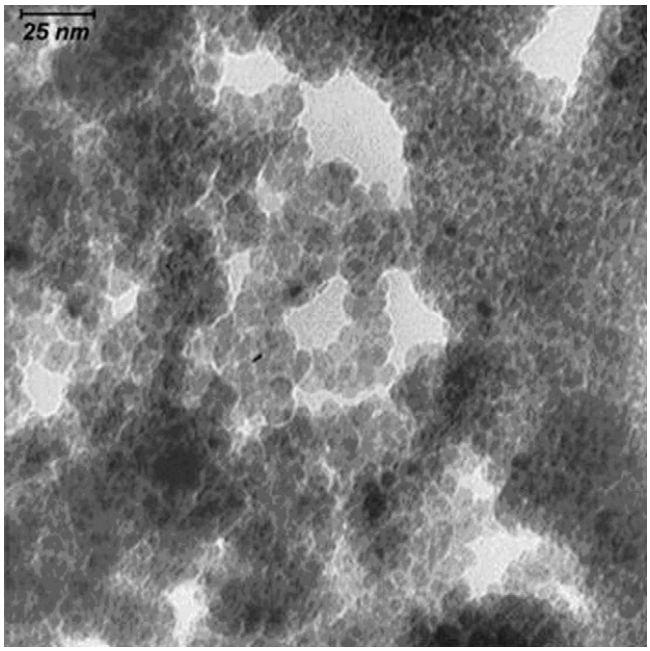

Fig. 8. TEM image of hausmannite (Mn_3O_4) (water/almond oil emulsion).

4. Conclusion

This study has demonstrated that manganese acetate is a proper precursor for the formation of Mn_3O_4 nanoparticles. The synthesis was carried out under normal condition and without any additives by applying ultrasonic waves in different media. The results show that the size and shape of the nanoparticles depends on the type of medium and the same product was formed in different media. The XRD patterns confirm that the ultrasound can crystallize the product without calcination. The higher crystallinity was found when the continuous phase was water or mineral oil. Ultrasound itself generates strong forces for proper dispersion of oil phases in water. The droplets act as a reactor for the formation of the product and affected the shape and size of the nanoparticles.

Acknowledgment

The financial support of the National Petrochemical industries Company of Iran (Project No. 0871886081) for doctoral project of Mrs Rohani was appreciated.

References

[1] G.A. Mansoori, T.A.F. Soelaiman, Nanotechnology—an introduction for the standards community, J. ASTM Int. 2 (2005) 21.
[2] G.A. Mansoori, Nanotechnology: the emerging cutting-edge technology, United Nations Tech. Monit. 53 (Special Issue) (2002).
[3] W. Wang, L. Ao, Synthesis and optical properties of Mn_3O_4 nanowires by decomposing $MnCO_3$ nanoparticles in flux, Cryst. Growth Des. 8 (2008) 358–362.
[4] W. Shen, F.E. Huggins, N. Shah, G. Jacobs, Y. Wang, X. Shi, G.P. Huffman, Novel Fe–Ni nanoparticle catalyst for the production of CO- and CO_2-free H_2 and carbon nanotubes by dehydrogenation of methane, Appl. Catal. A: Gen. 351 (2008) 102–110.
[5] A. Zolfaghari, F. Ataherian, M. Ghaemi, A. Gholami, Capacitive behavior of nanostructured MnO_2 prepared by sonochemistry method, Electrochim. Acta 52 (2007) 2806–2814.
[6] K.S. Suslick, Y. Didenko, M.M. Fang, T. Hyeon, K.J. Kolbeck, W.B. McNamara, M.M. Mdleleni, M. Wong, Acoustic cavitation and its chemical consequences, Phil. Trans. R. Soc. Lond. A 357 (1999) 335–353.
[7] H.G. Flynn, Physics of acoustic cavitation (A), J. Acoust. Soc. Am. 31 (1959) 1582–11582.
[8] A. Weissler, Formation of hydrogen peroxide by ultrasonic waves: free radicals, J. Am. Chem. Soc. 81 (1950) 1077–1081.
[9] K. Makino, M.M. Mossoba, P. Riesz, Chemical effects of ultrasound on aqueous solutions. Evidence for.OH and.H by spin trapping, J. Am. Chem. Soc. 104 (1982) 3537–3539.
[10] K.S. Suslick, S.-B. Choe, A.A. Cichowlas, M.W. Grinstaff, Sonochemical synthesis of amorphous iron, Nature 353 (1991) 414–416.
[11] K.S. Suslick, Sonochemistry, Science 247 (1990) 1439–1445.
[12] K. Okitsu, M. Ashokkumar, F. Grieser, Sonochemical synthesis of gold nanoparticles: effects of ultrasound frequency, J. Phys. Chem. B 109 (2005) 20673–20675.
[13] G. Kataby, Y. Koltypin, A. Ulman, I. Felner, A. Gedanken, Blocking temperatures of amorphous iron nanoparticles coated by various surfactants, Appl. Surf. Sci. 201 (2002) 191–195.
[14] R.A. Caruso, M. Ashokkumar, F. Grieser, Sonochemical formation of colloidal platinum, Colloids Surf. A 169 (2000) 219–225.
[15] N. Perkas, G. Amirian, C. Rottman, F. de la Vega, A. Gedanken, Sonochemical deposition of magnetite on silver nanocrystals, Ultrason. Sonochem. 16 (2009) 132–135.
[16] H. Xu, K.S. Suslick, Sonochemical synthesis of highly fluorescent Ag nanoclusters, ACS Nano (2010).
[17] S.H. Sonawane, B.M. Teo, A. Brotchie, F. Grieser, M. Ashokkumar, Sonochemical synthesis of ZnO encapsulated functional nanolatex and its anticorrosive performance, Ind. Eng. Chem. Res. 49 (2010) 2200–2205.
[18] H.-B. Pan, C.M. Wai, Sonochemical one-pot synthesis of carbon nanotube-supported rhodium nanoparticles for room-temperature hydrogenation of arenes, Phys. Chem. C 113 (2009) 19782–19788.
[19] M. Sivakumar, A. Towata, K. Yasui, T. Tuziuti, Y. Iida, A new ultrasonic cavitation approach for the synthesis of zinc ferrite nanocrystals, Curr. Appl. Phys. 6 (2006) 591–593.
[20] S. Avivi, Y. Mastai, A. Gedanken, Sonohydrolysis of In^{3+} ions: formation of needlelike particles of indium hydroxide, Chem. Mater. 12 (2000) 1229–1233.
[21] K. Vinodgopal, Y. He, M. Ashokkumar, F. Grieser, Sonochemically prepared platinum–ruthenium bimetallic nanoparticles, J. Phys. Chem. B 110 (2006) 3849–3852.
[22] S. Liu, L. Yin, Y. Koltypina, A. Gedankena, X. Xu, Y. Yeshurun, I. Felner, G. Gorodetsky, Preparation and magnetic properties of Fe–Ag granular alloy, J. Magn. Magn. Mater. 233 (2001) 195–204.
[23] D.N. Srivastava, N. Perkas, G.A. Seisenbaeva, Y. Koltypin, V.G. Kessler, A. Gedanken, Preparation of porous cobalt and nickel oxides from corresponding alkoxides using a sonochemical technique and its application as a catalyst in the oxidation of hydrocarbons, Ultrason. Sonochem. 10 (2003) 1–9.
[24] S.B. Parker, McGraw-Hill Encyclopedia of Chemistry, 5th ed., McGraw Hill, Inc., New York, 1983.
[25] E.R. Stobble, B.A. Boer, J.W. Geus, The reduction and oxidation behaviour of manganese oxides, Catal. Today 47 (1999) 161–167.
[26] W. Weimin, Y. Yongnian, Z. Jiayu, Selective reduction of nitrobenzene to nitrosobenzene over different kinds of trimanganese tetroxide catalysts, Appl. Catal. A 133 (1995) 81–93.
[27] E.J. Grootendorst, Y. Verbeek, V. Ponec, The role of the mars and van krevelen mechanism in the selective oxidation of nitrosobenzene and the deoxygenation of nitrobenzene on oxidic catalysts, J. Catal. 157 (1995) 706–712.
[28] T. Yamashita, A. Vannice, NO decomposition over Mn_2O_3 and Mn_3O_4, J. Catal. 163 (1996) 158–168.
[29] M. Baldia, F. Milellab, G. Ramisb, V.S. Escribano, G. Bu, An FT-IR and flow reactor study of the selective catalytic oxy-dehydrogenation of C3 alcohols on Mn_3O_4, Appl. Catal. A 166 (1998) 75–88.
[30] M. Anilkumar, V. Ravi, Synthesis of nanocrystalline Mn_3O_4 at 100 °C, Mater. Res. Bull. 40 (2005) 605–606.
[31] J. Mu, Z. Gu, Z. Zhang, X. Li, S.-Z. Kang, L. Wang, Effect of hydrothermal on the crystalline phase and morphology of manganese oxide nanocrystals, J. Dispersion Sci. Technol. 27 (2006) 1223–1225.
[32] J. Pike, J. Hanson, L. Zhang, S.-W. Chan, Synthesis and redox behavior of nanocrystalline hausmannite (Mn_3O_4), Chem. Mater. 19 (2007) 5609–5616.
[33] I. Djerdj, D. Arcon, Z. Jaglicic, M. Niederberger, Nonaqueous synthesis of manganese oxide nanoparticles, structural characterization, and magnetic properties, J. Phys. Chem. C 111 (2007) 3614–3623.
[34] P. Gibot, L. Laffont, Hydrophilic and hydrophobic nano-sized Mn_3O_4 particles, J. Solid State Chem. 180 (2007) 695–701.
[35] J. Mu, Z. Gu, H. Sun, Q. Wei, Low temperature synthesis of Mn_3O_4 nanoparticles using starch as cappingagent, J. Dispersion Sci. Technol. 27 (2006) 307–309.
[36] V. Ganesh Kumar, D. Aurbuch, A. Gedanken, A comparison between hot-hydrolysis and sonolysis of various Mn(II) salts, Ultrason. Sonochem. 10 (2003) 17–23.
[37] T.J. Mason (Ed.), Advances in Sonochemistry, vol. 3, JAI Press, London, 1993.
[38] R. Vijaya Kumar, Y. Diamant, A. Gedanken, Sonochemical synthesis and characterization of nanometer-size transition metal oxides from metal acetates, Chem. Mater. 12 (2000) 2301–2305.
[39] K. Okitsu, K. Iwasaki, Y. Yobiko, H. Bandow, R. Nishimura, Y. Maeda, Sonochemical degradation of azo dyes in aqueous solution: a new heterogeneous kinetics model taking into account the local concentration of OH radicals and azo dyes, Ultrason. Sonochem. 12 (2005) 255–262.
[40] http://www.diracdelta.com/.
[41] D.V. Talapin, A.L. Rogach, M. Haase, H. Weller, Evolution of an ensemble of nanoparticles in a colloidal solution: theoretical study, J. Phys. Chem. B 195 (2001) 12278–12285.
[42] E.V. Shevchenko, D.V. Talapin, H. Schnablegger, A. Kornowski, O. Festin, P. Svedlindh, M. Haase, H. Weller, Study of nucleation and growth in the organometallic synthesis of magnetic alloy nanocrystals: the role of nucleation rate in size control of $CoPt_3$ nanocrystals, J. Am. Chem. Soc. 125 (2003) 9090–9101.